

**Two-dimensional quantum diffusion of Gd adatoms in nano-size Fe corrals**R. X. Cao,<sup>1</sup> B. F. Miao,<sup>1</sup> Z. F. Zhong,<sup>1</sup> L. Sun,<sup>1</sup> B. You,<sup>1</sup> W. Zhang,<sup>1</sup> D. Wu,<sup>1</sup> An Hu,<sup>1</sup>  
S. D. Bader,<sup>2</sup> and H. F. Ding<sup>1,\*</sup><sup>1</sup>*National Laboratory of Solid State Microstructures and Department of Physics, Nanjing University,  
22 Hankou Road, Nanjing 210093, China*<sup>2</sup>*Materials Science Division and Center for Nanoscale Materials, Argonne National Laboratory,  
9700 South Cass Avenue, Argonne, Illinois 60439, USA*

(Received 12 August 2012; published 13 February 2013)

Gd atom diffusion in 30-nm-diameter Fe quantum corrals is studied utilizing scanning tunneling microscopy and kinetic Monte Carlo (KMC) simulations. The Gd adatom probability distribution inside the corral forms several trajectories and is closely related to oscillations of the local density of states at the Fermi level, as revealed by spectroscopy measurements. With increasing coverage, the Gd adatoms form a ringlike structure within the vicinity of the quantum corrals. The results are explained with KMC calculations utilizing experimentally determined long-range interactions and quantum confinement. The findings demonstrate that the diffusion of Gd adatoms is significantly influenced by the quantum corrals and that novel quantum ring structures can be created via control of the coverage.

DOI: [10.1103/PhysRevB.87.085415](https://doi.org/10.1103/PhysRevB.87.085415)

PACS number(s): 81.07.-b, 68.37.Ef, 73.21.-b, 81.16.Dn

**I. INTRODUCTION**

One of the beauties of nanoscience is the emergence of the quantum size effect (QSE) as the system size is reduced. The QSE has been demonstrated to influence various properties, such as atom diffusion,<sup>1,2</sup> growth stability,<sup>3-9</sup> optics,<sup>10</sup> magnetism,<sup>11-13</sup> transport,<sup>14</sup> and superconductivity.<sup>15</sup> The QSE in films is focused on confinement in one dimension (1D), the vertical direction. When electrons are confined in two dimensions (2D), one might expect even more novel phenomena to appear. Pioneering work has shown that electronic states confined in a nano-corral are dominated by the eigenstate density of electrons trapped in a round 2D quantum box.<sup>16</sup> Quantum interference also occurs on nano-size islands and vacancy islands.<sup>17,18</sup> The property influence by QSE has been less studied in 2D than 1D. Recently, quantum confinement in magnetic nano-islands was found to induce oscillations of the spin polarization of the local density of states (LDOS).<sup>19,20</sup> Theoretically, the 2D QSE was proposed to influence atom diffusion and self-organization.<sup>21</sup>

In this paper, we experimentally demonstrate that the 2D QSE can be used to tailor atomic diffusion within a nano-corral and create novel atomic-scale structures, such as quantum rings. We utilize atomic manipulation to build circular (30-nm diameter) quantum corrals on Ag(111) surfaces with Fe adatoms. Scanning tunneling spectroscopy measurements of the circular corrals' LDOS around the Fermi energy  $E_F$  show concentric standing waves, as revealed previously.<sup>16</sup> A few Gd atoms are introduced into the corrals, and the motions of these atoms are studied. The statistics reveal that the Gd adatom probability distribution inside the corral forms several trajectories and is closely related to oscillations of the LDOS at  $E_F$ . By tuning the Gd coverage, novel self-organized Gd quantum rings are formed in the vicinity of the Fe quantum corrals. The findings demonstrate that 2D quantum confinement can be used to engineer atom diffusion and build novel atomic structures.

**II. EXPERIMENTAL TECHNIQUES**

The experiments were performed in an ultrahigh vacuum chamber ( $2 \times 10^{-11}$  mbar) equipped with a low-temperature scanning tunneling microscope (STM) and a sputter gun. The surface of a high-purity Ag(111) crystal was cleaned by repeated cycles of argon ion sputtering (at 1.5 keV) and annealing (at 870 K). After that, the crystal was transferred into the STM stage and cooled to 4.7 K. High-purity Fe and Gd were deposited by means of electron beam evaporation onto the Ag(111) substrate in the STM stage at  $\approx 6$  K from outgassed rods. The typical rate of deposition was 0.002 monolayer/min. Electrochemically etched tungsten tips were used for the STM measurements. The bias voltage  $U$  refers to the sample voltage with respect to the tip. Spectroscopy measurements were performed via the modulation technique utilizing a 4-mV amplitude and 6.09-kHz frequency.

**III. RESULTS AND DISCUSSION**

We chose Fe adatoms as the building blocks of the quantum corrals because of the favorable diffusion barrier of  $\approx 43$  meV for Fe on Ag(111).<sup>22</sup> With this magnitude barrier, atomic manipulation can be readily achieved, while the adatoms can then be immobilized after positioning at 4.7 K. No apparent change of the corral shape is found for temperatures  $< 14$  K. About 0.001 monolayer equivalents (MLE) of single Fe adatoms were deposited. With stabilizing condition of  $-1$  V and 1 nA, the tip further approached the sample surface within a distance of  $\approx 0.4$  nm to drive the Fe adatoms to the designed positions. Figure 1(a) shows a typical circular quantum corral with 30-nm diameter. The Ag(111) surface contains a 2D electron gas. These electrons inhabit a surface-state band that starts at 67 meV below  $E_F$ .<sup>23</sup> Surface-state electrons are confined within the corral by strong scattering at the corral walls leading to a concentric circular standing-wave pattern, as shown in Fig. 1(b) for energy near  $E_F$ . An average line profile from the center to the Fe circle, indicated by the black

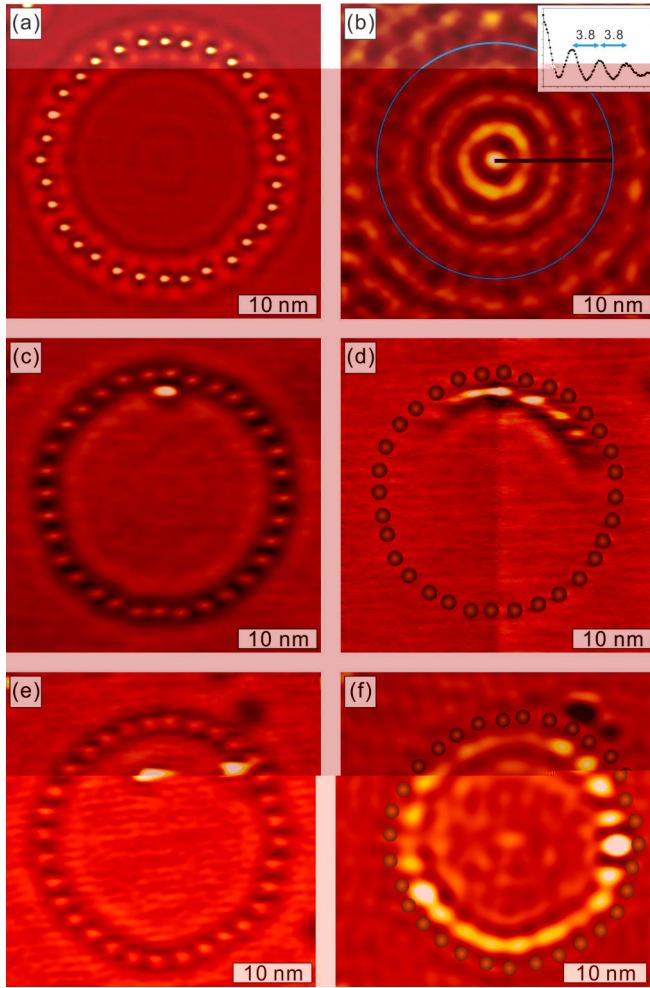


FIG. 1. (Color online) (a) STM topography of circular corral built with 32 Fe adatoms on Ag(111) ( $U = 100$  mV,  $I_t = 1$  nA). (b) LDOS near  $E_F$  inside the corral ( $U = 20$  mV,  $I_t = 1$  nA). Fe circular corral is indicated by blue circle for clarity. Inset: Average period of standing wave indicated by black line in (b) is  $\approx 3.8$  nm, which corresponds to half of the Fermi wavelength of Ag(111). (c) and (e) Typical STM image of one and two Gd adatoms inside a corral, respectively. (d) and (f) The probability distribution of one and two Gd adatoms in a circular corral, respectively. For clarity, small balls are added to mark the positions of Fe adatoms.

line, is plotted in the inset of Fig. 1(b). The average period of the standing wave is  $\approx 3.8$  nm, which corresponds to half of the Fermi wavelength of the Ag(111) surface state. The concentric circular pattern suggests the possibility to control atom diffusion and create novel atomic structures via 2D quantum confinement.

Gd was chosen to study the adatom diffusion inside the quantum corrals because Gd is of general interest due to its large magnetic moment. We find experimentally that Gd adatoms can form a well-ordered superlattice on Ag(111) flat terraces, similar to the Ce/Ag(111) system.<sup>24</sup> The superlattice is formed by long-range interaction (LRI) via surface state electrons.<sup>24–27</sup> About 0.02% MLE of Gd adatoms were deposited on the prepatterned Ag(111) surface. Then adatom diffusion on flat terraces and inside the corrals was studied. Temperature-dependent measurements of single adatom

diffusion show that Gd adatoms have a diffusion barrier of  $\approx 7.6$  meV and attempt frequency of  $\approx 2 \times 10^9$  Hz on Ag(111), so they are mobile and difficult to observe above 4.7 K. Hence, we cooled the system to  $< 4.4$  K for the diffusion studies. To minimize tip-induced atomic motion, we chose tunneling conditions of  $-50$  mV and 2 pA for imaging. (With this condition, we hardly observe any single-step adatom hopping below 3.4 K.) On a flat terrace without quantum corrals, we find the Gd adatoms follow a 2D random walk, similar to that observed for the diffusion of Cu single adatoms on a flat Cu(111) surface.<sup>2</sup> Figure 1(c) presents a typical image of one adatom inside a circular corral. The Gd atoms appear to be larger than the Fe atoms, which is partly attributable to Gd movement during the imaging. To obtain statistics on the Gd diffusion inside the corral, we continued to image the same area until the liquid He in the cryostat evaporated. We collected consecutive images (Supplementary Material S1<sup>28</sup>) and averaged them into a single image. With further background subtraction to remove the electronic effect caused by the corral, the statistical result is shown in Fig. 1(d). We note that the standing wave caused by the Gd adatoms remains as Gd adatoms move. For this reason the surrounding area of the arc appears dark. We find that the adatoms mostly stay in the vicinity of a specific location and form an arc-shaped distribution near one side of the Fe corral, which is in contrast to theoretically predicted circular orbits.<sup>21</sup> This may be due to the fact that the Fe adatoms in the experiments are not positioned in as perfect a circle as in the theory resulting in preferred occupation sites. To verify this, we repeated the measurements with new corrals and found that the arcs are always located near one side of the corral, but at different locations for different experiments. The random distribution of arcs suggests they are preferred occupation sites.

To overcome the problem of Gd adatom trapping at preferred occupation sites, we studied the diffusion of pairs of Gd adatoms inside a quantum corral. The idea was to use the collision of two adatoms to kick an adatom out of the preferred occupation site where it was trapped. Figure 1(e) presents a typical image of two adatoms inside a circular corral. We collected 510 images (Supplementary Material S2<sup>28</sup>); the statistical result is shown in Fig. 1(f). The averaged image shows three concentric orbits of adatom motion and one focused at the center. The orbits have different intensities, suggesting that they have different occupancies. Brighter orbits signify higher occupancy. The outermost orbit of Fig. 1(f) has a few bright spots of high probability. The appearance of the bright spots relates to the observation of the preferred occupation sites for the single adatom diffusion. We note that the depressions beside the bright spots are caused by the standing wave of the Gd adatoms which is difficult to be removed.

In order to compare with experiment, we performed kinetic Monte Carlo (KMC) calculations to simulate the diffusion process of one and two Gd adatoms inside the corral. The method had been used previously for the simulation of Fe superlattice formation on Cu(111).<sup>22</sup> In the simulations, the hopping rate of an adatom from site  $i$  to site  $j$  on the Ag(111) surface is calculated using the expression  $v_{i \rightarrow j} = v_0 \exp(-E_{i \rightarrow j}/k_B T)$ , where  $T$  is the temperature of the substrate,  $v_0$  is the attempt frequency,  $k_B$  is the Boltzmann

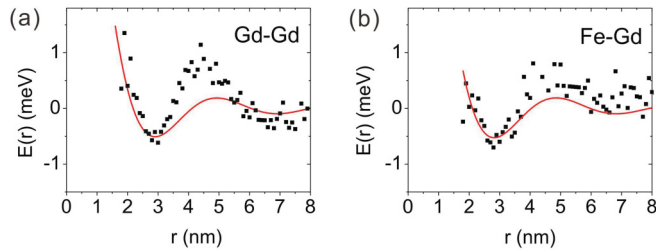


FIG. 2. (Color online) Long-range interaction between (a) two Gd atoms and (b) Gd-Fe single adatoms on Ag(111). Symbols are experimental data of nearest-neighbor separation distribution, and lines are the fit mentioned in the text.

constant, and  $E_{i \rightarrow j}$  is the hopping barrier. The influence of the LRI via surface state electrons is included in the hopping barrier, i.e.  $E_{i \rightarrow j} = E_d + 0.5(E_j - E_i)$ , where  $E_d$  is the diffusion barrier for an isolated atom on a clean surface, and  $E_i(E_j)$  is the total energy caused by the LRI. The LRI between Gd-Gd and Fe-Gd are obtained from a combination of experimental results (Fig. 2) and the fitted curve using the theoretical model of interaction mediated by a Shockley surface-state band.<sup>26</sup>

Utilizing the LRI between Fe and Gd atoms, the potential distribution inside the circular corral is calculated by summing up all contributions from the 32 Fe atoms [Fig. 3(a)]. The experimental values are used when the atomic separation is  $< 5$  nm; otherwise, the fitted potential is used. The line profile in the LRI map, marked as a blue line, is shown in Fig. 3(b). It has the same periodicity, 3.8 nm, as the LDOS shown in Fig. 1(a). With this, we also computed the probability distribution for two Gd adatoms inside the corral [Fig. 3(c)]. It shows three concentric orbits and one focused center, in agreement with the experimental findings. We note that we did not find any apparent difference between the probability distribution for single Gd-adatom or two-adatom diffusion when the Fe adatoms are positioned almost as a perfect circle. To make a more quantitative comparison, we plot both the experimental (red column) and simulated (black curve) radial distributions of the visiting probability in Fig. 3(d). Both datasets show four peaks with almost the same peak positions. The separations between the peaks are all  $\approx 3.8$  nm. The difference in the intensities of these peaks may be due to the fact that the Fe adatoms are not as ideally positioned as they are in the simulations. (When we take the experimental positions of the Fe atoms as the calculation input, we can reproduce most of the preferred occupation sites yielding better agreement.) In addition, the experimental data are obtained from only 510 images, while the simulated data are the statistical result of  $10^8$  samplings. In comparison with the LDOS near  $E_F$  shown in Fig. 1(b), we note the similarity between the LDOS and the distribution of the adatom diffusion, which both show three concentric orbits and one focused at the center. The separations between the orbits are all  $\approx 3.8$  nm, which corresponds to half of the Fermi wavelength of the Ag(111) surface state. The similarity between the distribution of the adatom diffusion probability and the LDOS demonstrates that quantum confinement can significantly modify atomic diffusion.

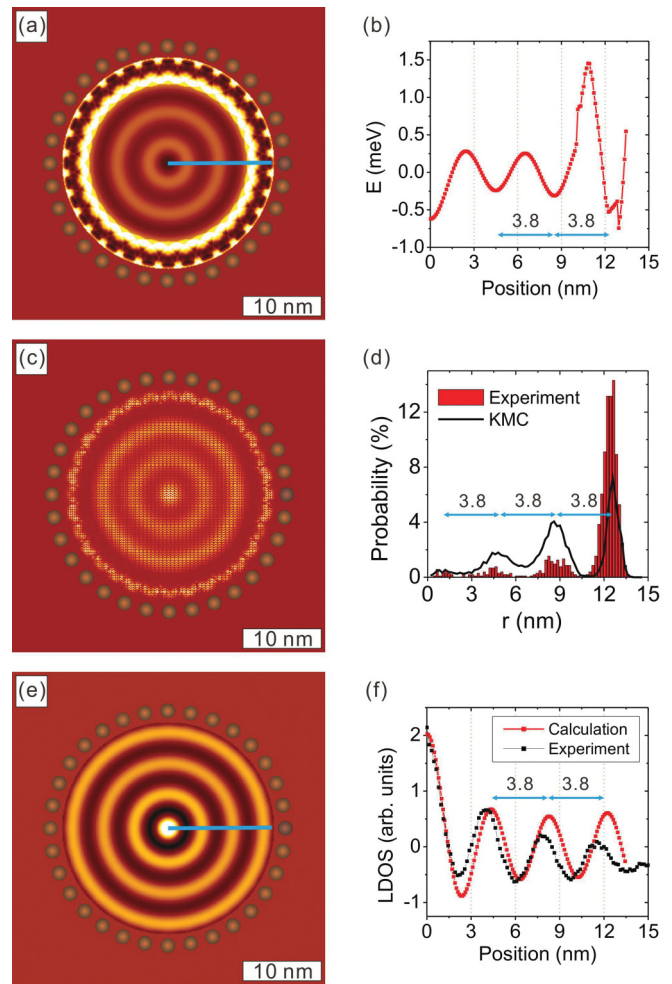


FIG. 3. (Color online) (a) Calculated interaction energy between a Gd atom and the circular corral. (b) The line profile marked in (a). (c) Adatom probability distribution of KMC simulations with  $10^8$  samplings. (d) Experimental histogram (red column) of the radial distributed probability and theoretical radial distribution (black line) obtained from KMC simulations. Note that the average period of 3.8 nm is observed in both distributions. (e) Calculated LDOS within a circular Fe corral (see text). (f) The line profile marked in (e) (red rectangles) and experimental LDOS distribution shown in the inset of Fig. 1(b) (black rectangles). Fe atoms are marked by small balls.

We also notice that the LDOS has its maximum at the center, while the Gd adatoms mostly stay at the orbit next to the Fe corral. This can be understood as follows. Electrons have dual particle-wave properties. When taken as a particle, the LDOS measurements inside a corral represent the statistics of electron motion inside the corral. We do not expect this would be the same for the statistics of a Gd adatom inside the corral because the interaction between an electron and the corral can differ from the surface-state-mediated interaction of an atom with the corral. For instance, they have different decay behavior. The LDOS decays inversely with the distance from the scattering center, i.e. the Fe adatoms.<sup>29</sup> The surface-state-mediated interaction between Gd and Fe adatoms, however, decays in an inverse square law as a function of separation.<sup>26</sup> In addition, they have different dependence on the phase shift. When taking these into account and summing up all the standing waves from

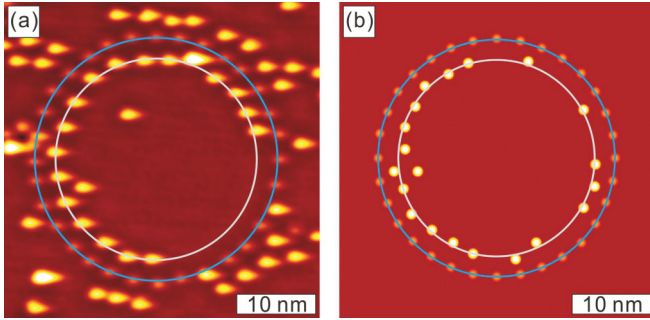


FIG. 4. (Color online) (a) Typical topography image of 20 Gd atoms inside a Fe circular corral. (b) KMC simulation of the same coverage.

the 32 individual Fe atoms with the formula given in Ref. 29, we find the LDOS indeed has its maximum at the corral center [Figs. 3(e) and 3(f)]. We note that the discrepancy between experiment and theory, see Fig. 3(f), is expected since multiple scattering is neglected in this simplified model. On the other hand, the computed interaction energy between a Gd adatom and the Fe corral has the lowest minimum at the orbit next to the corral [Figs. 3(a) and 3(b)]. There is also a high and asymmetric barrier separating this orbit and the other orbits. These two features make it most visited by the Gd adatoms, as observed experimentally.

The diffusion study shows that the orbit next to the corral has maximum occupancy for a Gd visit. When more Gd atoms are deposited, it would be expected that they would mostly locate at this orbit. Due to the surface-state-mediated LRI, they will separate from each other with a fixed separation to further lower the energy, and a ringlike structure will be formed. Figure 4(a) shows a typical image of 20 Gd adatoms inside the Fe corral. We find that most of the adatoms are indeed

located near the quantum corral, forming a ringlike structure. The Gd adatoms have a fixed separation of  $\approx 3$  nm, which is determined by the first minimum of the LRI shown in Fig. 2(a). These findings are supported by the KMC simulations shown in Fig. 4(b), where a ringlike structure is apparent. With repeated simulations, the ring appears at different locations, but most of the Gd adatoms are within the orbit next to the corral. Sometimes the ring also breaks into several segments, similar to that shown on the right side of Fig. 4(b). The appearance of the ringlike structures demonstrates the power of 2D quantum confinement to create novel atomic arrangements.

#### IV. SUMMARY

In summary, utilizing scanning tunneling microscopy and spectroscopy, we studied Gd atomic diffusion and its relation to the LDOS inside a 30-nm Fe quantum corral. The Gd adatom probability distribution inside the corral forms several trajectories and is closely related to oscillations of the LDOS at the Fermi level, as revealed by spectroscopy. With increasing Gd dosage, a ringlike structure is found within the vicinity of the corral. The findings demonstrate that 2D quantum confinement can be used to control atomic diffusion and to create novel atomic structures, such as quantum rings.

#### ACKNOWLEDGMENTS

Work at Nanjing was supported by the State Key Program for Basic Research of China (Grant No. 2010CB923401), NSFC (Grants Nos. 10834001, 10974087, and 11023002) and PAPD. Work at Argonne was supported by the US Department of Energy, Office of Science, Basic Energy Sciences, under Contract No. DE-AC02-06CH11357.

\*Corresponding author: hfding@nju.edu.cn

<sup>1</sup>L. Y. Ma, L. Tang, Z. L. Guan, K. He, K. An, X. C. Ma, J. F. Jia, Q. K. Xue, Y. Han, S. Huang, and F. Liu, *Phys. Rev. Lett.* **97**, 266102 (2006).

<sup>2</sup>N. N. Negulyaev, V. S. Stepanyuk, L. Niebergall, P. Bruno, W. Hergert, J. Repp, K. H. Rieder, and G. Meyer, *Phys. Rev. Lett.* **101**, 226601 (2008).

<sup>3</sup>B. J. Hinch, C. Koziol, J. P. Toennies, and G. Zhang, *Europhys. Lett.* **10**, 341 (1989).

<sup>4</sup>A. R. Smith, K. J. Chao, Q. Niu, and C. K. Shih, *Science* **273**, 226 (1996).

<sup>5</sup>L. Gavioli, K. R. Kimberlin, M. C. Tringides, J. F. Wendelken, and Z. Zhang, *Phys. Rev. Lett.* **82**, 129 (1999).

<sup>6</sup>V. Yeh, L. Berbil-Bautista, C. Z. Wang, K. M. Ho, and M. C. Tringides, *Phys. Rev. Lett.* **85**, 5158 (2000).

<sup>7</sup>D. A. Luh, T. Miller, J. J. Paggel, M. Y. Chou, and T. C. Chiang, *Science* **292**, 1131 (2001).

<sup>8</sup>M. M. Özer, Y. Jia, B. Wu, Z. Zhang, and H. H. Weitering, *Phys. Rev. B* **72**, 113409 (2005).

<sup>9</sup>Z. Zhang, Q. Niu, and C. K. Shih, *Phys. Rev. Lett.* **80**, 5381 (1998).

<sup>10</sup>F. Hache, D. Ricard, and C. Flytzanis, *J. Opt. Soc. Am. B* **3**, 1647 (1986).

<sup>11</sup>F. Liu, S. N. Khanna, and P. Jena, *Phys. Rev. B* **42**, 976 (1990).

<sup>12</sup>Z. Q. Qiu, J. Pearson, A. Berger, and S. D. Bader, *Phys. Rev. Lett.* **68**, 1398 (1992).

<sup>13</sup>J. Li, M. Przybylski, F. Yildiz, X. D. Ma, and Y. Z. Wu, *Phys. Rev. Lett.* **102**, 207206 (2009).

<sup>14</sup>N. D. Lang and P. Avouris, *Phys. Rev. Lett.* **81**, 3515 (1998).

<sup>15</sup>Y. Guo, Y. F. Zhang, X. Y. Bao, T. Z. Han, Z. Tang, L. X. Zhang, W. G. Zhu, E. G. Wang, Q. Niu, Z. Q. Qiu, J. F. Jia, Z. X. Zhao, and Q. K. Xue, *Science* **306**, 1915 (2004).

<sup>16</sup>M. F. Crommie, C. P. Lutz, and D. M. Eigler, *Science* **262**, 218 (1993).

<sup>17</sup>J. Li, W. D. Schneider, R. Berndt, and S. Crampin, *Phys. Rev. Lett.* **80**, 3332 (1998).

<sup>18</sup>L. Niebergall, G. Rodary, H. F. Ding, D. Sander, V. S. Stepanyuk, P. Bruno, and J. Kirschner, *Phys. Rev. B* **74**, 195436 (2006).

<sup>19</sup>O. Pietzsch, S. Okatov, A. Kubetzka, M. Bode, S. Heinze, A. Lichtenstein, and R. Wiesendanger, *Phys. Rev. Lett.* **96**, 237203 (2006).

- <sup>20</sup>H. Oka, P. A. Ignatiev, S. Wedekind, G. Rodary, L. Niebergall, V. S. Stepanyuk, D. Sander, and J. Kirschner, *Science* **327**, 843 (2010).
- <sup>21</sup>V. S. Stepanyuk, N. N. Negulyaev, L. Niebergall, R. C. Longo, and P. Bruno, *Phys. Rev. Lett.* **97**, 186403 (2006).
- <sup>22</sup>X. P. Zhang, B. F. Miao, L. Sun, C. L. Gao, A. Hu, H. F. Ding, and J. Kirschner, *Phys. Rev. B* **81**, 125438 (2010).
- <sup>23</sup>J. Li, W. D. Schneider, and R. Berndt, *Phys. Rev. B* **56**, 7656 (1997).
- <sup>24</sup>F. Silly, M. Pivetta, M. Ternes, F. Patthey, J. P. Pelz, and W. D. Schneider, *Phys. Rev. Lett.* **92**, 016101 (2004).
- <sup>25</sup>K. H. Lau and W. Kohn, *Surf. Sci.* **75**, 69 (1978).
- <sup>26</sup>P. Hylgaard and M. Persson, *J. Phys.: Condens. Matter* **12**, L13 (2000).
- <sup>27</sup>N. Knorr, H. Brune, M. Epple, A. Hirstein, M. A. Schneider, and K. Kern, *Phys. Rev. B* **65**, 115420 (2002).
- <sup>28</sup>See Supplemental Material at <http://link.aps.org/supplemental/10.1103/PhysRevB.87.085415> for S1, consecutive images of the diffusion of one Gd adatom inside a 30-nm Fe corral; S2, consecutive images of the diffusion of two Gd adatoms inside a 30-nm Fe corral.
- <sup>29</sup>M. F. Crommie, C. P. Lutz, and D. M. Eigler, *Nature* **363**, 524 (1993).